

The Comparative of α - and β -Cyclodextrin as Stabilizing Agents on AuNPs and Application as Colorimetric Sensors for Fe^{3+} in Tap Water

Adhi Maulana Yusuf^{1,2}, Satrio Kuntolaksono², and Agustina Sus Andreani^{1*}

¹Research Centre for Chemistry, National Research and Innovation Agency (BRIN), Kawasan Puspiptek, Building 452, Serpong, Banten 15314, Indonesia

²Department of Chemical Engineering, Institut Teknologi Indonesia, Jl. Raya Puspiptek, Serpong, Banten 15314, Indonesia

* Corresponding author:

email: agus147@brin.go.id

Received: April 10, 2023

Accepted: July 17, 2023

DOI: 10.22146/ijc.83796

Abstract: In this study, AuNPs were reduced using ortho-hydroxybenzoic acid (o-HBA) and various stabilizing agents (α -CDs and β -CDs). The stability, shape, size, and sensitivity of the Fe^{3+} detection of AuNPs α -CDs and AuNP β -CDs are compared. Both nanomaterials were characterized using ultraviolet-visible (UV-vis) spectroscopy, Fourier transform infrared (FTIR) spectroscopy, and transmission electron microscopes (TEM). After the addition of Fe^{3+} , the absorption rate of surface plasma resonance (SPR) increased to 524 nm, and the color of AuNPs α -CDs and AuNPs β -CDs was changed from pink to red and purple, respectively. AuNPs α -CDs are more uniform in shape and size than AuNPs β -CDs with a size of 23.34 nm. Further, AuNPs α -CDs are more stable, and the absorption rate at 524 nm wavelength decreases by 17.76%. AuNPs α -CDs have a good linear relationship with a linear regression coefficient of 0.996. The sensitivity of AuNPs α -CDs was good with LoD and LoQ both with 1.21 and 4.02 ppm, respectively. These results show that the sensor is superior in determining Fe^{3+} . In addition, AuNPs α -CDs were used to detect Fe^{3+} in the tap water in South Tangerang, Banten, Indonesia.

Keywords: AuNPs α -CDs; AuNPs β -CDs; colorimetric detection; Fe^{3+} ; tap water

■ INTRODUCTION

Heavy metals have become the most dangerous chemical for water bodies, soil, and air due to the growth of contemporary industry [1]. Heavy metals are non-biodegradable and cannot be digested, therefore, they will be accumulated in living organisms after entering their food chain [2] which has become an issue due to their significant impact on environmental and health problems [3]. An example of a toxic heavy metal is elemental iron (Fe). Fe element is the most important element and is also important in the natural environment [4]. Ion Fe^{3+} plays critical roles in many pathological and physiological processes, including cell metabolism, enzyme catalysis, nucleic acid synthesis, and electron transport [5]. Neither excess accumulation nor lack of Fe^{3+} leads to several diseases, such as cancer, Parkinson's syndrome, Alzheimer's disease, and anemia [6-7]. Therefore, it must

be controlled at a significant level to avoid disease. This condition has been driving researchers and academicians to focus on constructive methods for the qualitative and quantitative detection of Fe^{3+} ions [8]. On the other hand, several methods have been developed for the determination of Fe^{3+} , including inductively coupled plasma mass spectroscopy (ICP-MS) [9], high-performance liquid chromatography (HPLC) [10], atomic absorption spectroscopy (AAS) [11], fluorescence spectroscopic analysis [12], electrochemical methods [13], and UV-visible spectrophotometer [14]. However, these methods require advanced equipment, technical expertise, and need time for sample preparation steps. Therefore, it is thought that these techniques are not economical and user-friendly. In order to overcome these disadvantages, the colorimetric method has been developed for the detection of metal ions in aqueous solutions [15]. Nowadays, metallic nanoparticle sensors

have been widely used for colorimetric detection of Fe^{3+} ions due to their strong surface plasmon resonance (SPR), stable dispersion, biocompatibility, and controllable physical/chemical properties [16]. Due to this reason, colorimetric sensors are the best way to detect Fe^{3+} ions.

In recent years, gold nanoparticles (AuNPs) have attracted a lot of attention as research materials recently and have been widely used in a wide range of applications, such as sensing, electronics, surface-enhanced Raman spectroscopy, drug delivery, bioimaging, catalysis, colorimetric sensors, gene therapy, and so on [17]. The AuNPs exhibit specific optical characteristics in the 380–750 nm wavelength region (visible region). The SPR phenomenon is the result of surface plasmon confinement near a nanoparticle in which the size of the nanoparticle is smaller than the wavelength of incident light; this is known as the optical characteristics of the metallic nanoparticles. This phenomenon stems from the coherent oscillation of the surface conduction electrons excited by electromagnetic radiation. This phenomenon can be found in materials with a negative real and small positive imaginary dielectric constant [18]. The mechanism of SPR sensors is based on the sensitivity of the frequency of the oscillating electron to the environment of the plasmonic nanoparticles [19]. The dependency of frequency and intensity of the surface plasmon resonance adsorption bands on the type, shape, size, and size distribution of the nanoparticles provide a wide variety of sensing applications [20]. Additionally, AuNPs can be used to provide a method for detecting iron concentration in tap water samples.

Cyclodextrins (CDs) are cyclic oligosaccharides consisting of (α -1,4)-linked D-glucopyranose units. The most common natural CDs and the only ones used in pharmaceutical products are α -CDs and β -CDs consisting of 6 and 7 D-glucopyranose units. The α -CDs and β -CDs are doughnut-shaped molecules with a hydrophilic outer surface and a slightly lipophilic central cavity. The outside of the CDs toroid is hydrophilic due to the hydroxyl groups, giving the molecules with good water solubility, whereas the inside is relatively hydrophobic because of the glycosidic oxygen bridges [21]. CDs are non-toxic, biodegradable and biocompatible, along with the

collective effects of inclusion, size specificity, controlled release capability, and transport properties, making them suitable as host molecules [22].

Both α - and β -CDs can be used as the stabilizing agent to synthesize AuNPs. For instance, the work of Gopalan [23] using β -CDs to stabilize metal nanoparticles (AuNPs and AgNPs), concluding gold and silver nanoparticles are relatively stable and make it possible to control the size and distribution of the nanoparticles using β -CDs as a stabilizer. Also, Liu et al. [24] report control of the size and distribution of AuNPs were synthesized by the reduction of hydrogen tetrachloroaurate(III) trihydrate by sodium citrate and different CDs (α -, β - and γ -) used as the stabilizer, concluding the main reason for why cyclodextrins stabilize gold colloids is considered to be hydrophobic-hydrophobic interactions between CDs and AuNPs. The work of Lakkakula et al. [25] synthesized gold nanoclusters using β -CDs to stabilize for bioimaging and selective label-free intracellular sensing of Co^{2+} ions, concluding highly selective, rapid detection method using gold nanoclusters stabilized by CD and highly biocompatible with did not affect cell growth phases. Furthermore, Co^{2+} can be detected fast (within 5 min) with high sensitivity and selectivity.

In this study, we described the fabrication of AuNPs using *ortho*-hydroxybenzoic acid (*o*-HBA) with α -CDs and β -CDs, namely AuNPs α -CDs and AuNPs β -CDs. The *o*-HBA contains hydroxyl phenolic and carboxylate functional groups that would be suitable to act as reducing. Furthermore, we also compare the synthesis of AuNPs with a combination of α -CDs and β -CDs to act as stabilizers to obtain stability, sensitivity, selectivity, LoD (limit of detection), and LoQ (limit of quantitation). In the last, AuNPs combination with α -CDs was utilized to determine Fe^{3+} in tap waters.

■ EXPERIMENTAL SECTION

Materials

The materials used in this study were *o*-hydroxybenzoic acid from Central Drug House, New Delhi, India. α -CDs, β -CDs, sodium hydroxide, HAuCl_4 , and ethylenediaminetetraacetic acid (EDTA) were

purchased from Sigma-Aldrich. The standard solutions like Fe^{3+} , Ni^{2+} , Cd^{2+} , Pb^{2+} , Cu^{2+} , Sn^{2+} , Co^{2+} , and Mg^{2+} were obtained from Merck KGaA, Darmstadt, Germany. HCl and HNO_3 were purchased from Mallinckrodt. All these chemical agents were used as received.

Instrumentation

The instrumentations used in this study were ultraviolet-visible (UV-vis) spectra using Agilent Cary 60 UV-vis spectroscopy between 200–800 nm range. The size distribution and morphology of nanoparticles were analyzed by transmission electron microscope (TEM) Tecnai G2 20S-Twin Function. Fourier transform infrared spectroscopy (FTIR) spectra were measured using Shimadzu IR Prestige 21 in the 400–4000 cm^{-1} range. The Fe^{3+} content of the tap water samples was determined using an Agilent 280FS AA.

Procedure

Synthesis of AuNPs-CDs

The synthesis of AuNPs α -CDs and AuNPs β -CDs was carried out by mixing 100 ppm HAuCl_4 , 0.01 M *o*-HBA at pH 12, and a concentration of 0.02 M CDs (α or β) with the volume ratio of 1:1:1 in a water bath at 98 °C for 20 min.

Stability of AuNPs-CDs

The stability of AuNPs α -CDs and AuNPs β -CDs was carried out by storing the synthesized AuNPs for 3 months in the refrigerator at 4 °C, then examining them with UV-vis spectrometry to compare with the SPR spectra results of the AuNPs-CDs when they were synthesized.

Colorimetric response of AuNPs-CDs towards metals

The synthesized AuNPs α -CDs and AuNPs β -CDs were evaluated for their colorimetric response to Fe^{3+} , Mg^{2+} , Ni^{2+} , Cd^{2+} , Pb^{2+} , Cu^{2+} , Sn^{2+} , and Co^{2+} . One mL of 10 ppm heavy metal solution at room temperature was combined with 1 mL of AuNPs α -CDs and β -CDs synthesized under optimum conditions (100 ppm HAuCl_4 , 0.01 M *o*-HBA at pH 12, and 0.02 M α or β CDs with a 1:1:1 volume ratio). The combination was then shaken to homogenization and analyzed using UV-vis spectrometry.

Other metal ion interference in the reaction of AuNPs-CDs with Fe^{3+}

The interference is evaluated by including additional heavy metal ions in the AuNPs α -CDs + Fe^{3+} and AuNPs β -CDs + Fe^{3+} . One mL of Fe^{3+} (10 ppm) and 1 mL of each of the additional (10 ppm) heavy metal ions: Mg^{2+} , Ni^{2+} , Cd^{2+} , Pb^{2+} , Cu^{2+} , Sn^{2+} , and Co^{2+} were added to the mixture with a 2:1:1 volume ratio, which was then shaken to homogenization and subjected to UV-vis spectrometric analysis.

Analytical performance

For the calibration plot, the absorbance values at 524 nm versus the concentration of Fe^{3+} were applied. The LoD and LoQ were determined from three times the standard deviation of the blank signal and ten times the standard deviation of the blank signal, respectively [26]. The LoD and LoQ of the developed colorimetric sensor were calculated using Eq. (1) and (2):

$$\text{LoD} = 3 \times \frac{S_y}{a} \quad (1)$$

$$\text{LoQ} = 10 \times \frac{S_y}{a} \quad (2)$$

where S_y is the standard deviation, and a is the slope of the calibration curve, were used to estimate the LoD and LoQ with variation in concentration of Fe^{3+} (2, 6, 10, 14, 18 ppm). Three times of the detection Fe^{3+} standard solution analysis using AuNPs α -CDs and AuNPs β -CDs under ideal conditions were tested for repeatability and reproducibility. The spiking method was used to determine the accuracy parameters. In tap water, the measurement of the Fe^{3+} standard solution's recovery value was analyzed.

Reusability of AuNPs-CDs as Fe^{3+} colorimetric sensor

The reusability test was performed by introducing 1 mL of Fe^{3+} 10 ppm and 1 mL of EDTA 25 ppm to 1 mL of AuNPs α -CDs and adding 1 mL of EDTA 40 ppm to AuNPs β -CDs with a 1:1 volume ratio. The resulting mixture was then homogenized by shaking and analyzed using UV-vis spectrometry.

Application test to tap water

Three water samples collected from different tap water areas in South Tangerang, Banten, Indonesia, were filtered with 0.45 μm filter paper and preserved with

HNO₃ to pH < 2. Samples were analyzed by AAS to compare the results. The application test was performed by 1 mL samples added with 1 mL of AuNPs α -CDs analyzed by UV-vis spectrometry.

RESULTS AND DISCUSSION

Synthesis of AuNPs-CDs

o-HBA was chosen as the reducing agent of AuNPs due to its ability to convert Au³⁺ to Au⁰ with an optimization peak which is found in *o*-HBA at pH 12 [27]. α - and β -CDs were selected as a stabilizer because CDs are hollow compounds that have steric hindrance, so they can stabilize the nanoparticles. After the production of AuNPs α -CDs and β -CDs, the maximum wavelength for the SPR is detected at 524 nm which is included in the specific optical SPR of AuNPs in the wavelength region of 350–750 nm (visible region) [18] with an absorbance of 0.49 for AuNPs α -CDs and 0.51 for AuNPs β -CDs with the color of the resulting solution is bright pink (Fig. 1). The size of AuNPs α -CDs and β -CDs was relatively small because the SPR peak was sharp [28]. The size of AuNPs α -CDs and β -CDs was confirmed by the TEM.

The stability of AuNPs after 3 months of incubation of AuNPs α -CDs and AuNPs β -CDs in the refrigerator at 4 °C did not change the color solution. There is a decrease in absorbance at the same wavelength at 524 nm from 0.49 to 0.40 (17.76%) for AuNPs α -CDs and from 0.51 to 0.39 (22.95%) for AuNPs β -CDs. Thus, AuNPs α -CDs are

more stable than AuNPs β -CDs (Fig. 2).

After testing using TEM, the average results of nanoparticle size for AuNPs α -CDs and AuNPs β -CDs were 23.34 and 40.74 nm, respectively. The shape of the AuNPs α -CDs is spherical, and the shape of the AuNPs β -CDs is various (triangle, hexagon, and square). Thus, AuNPs α -CDs nanoparticles are more uniform in shape than AuNPs β -CDs (Fig. 3).

Colorimetric Response of AuNPs-CDs toward Metals

The comparison of AuNPs using different stabilizers of α -CDs and β -CDs with the presence of heavy

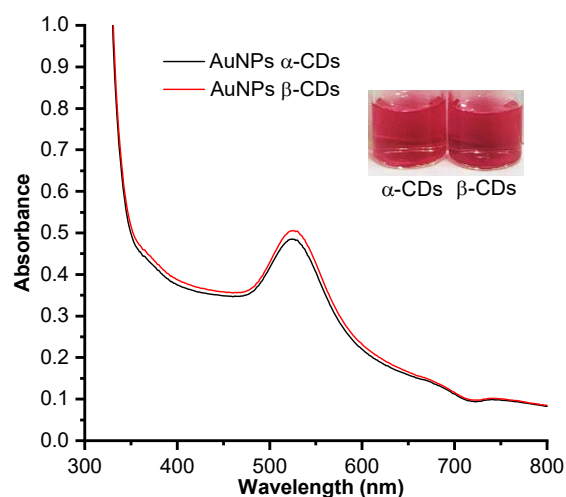


Fig 1. The UV-vis spectra of AuNPs α -CDs and AuNPs β -CDs with their color solution as inset

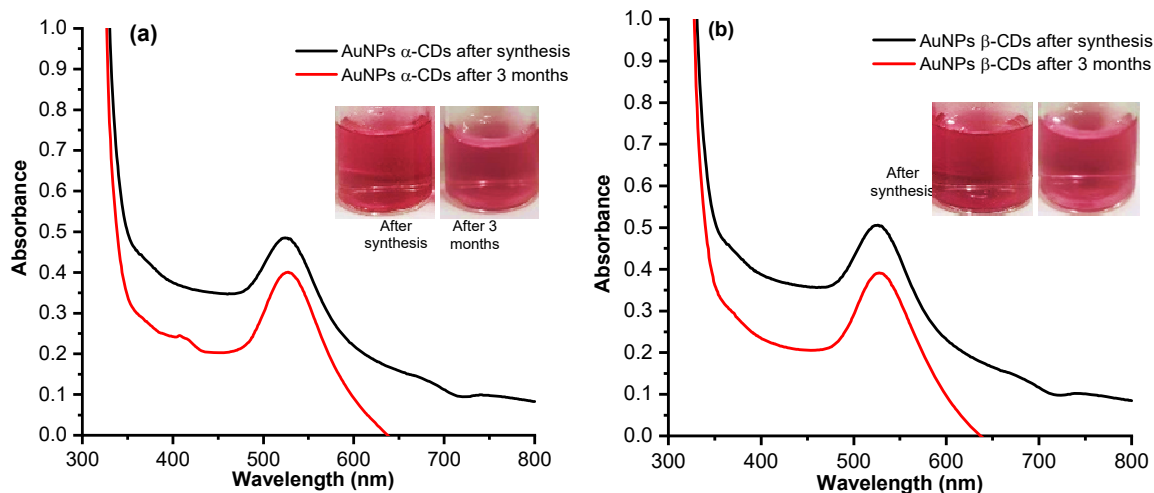


Fig 2. SPR spectra of the stability of AuNPs after 3 months incubation (a) AuNPs α -CDs and (b) AuNPs β -CDs with their color solution as inset

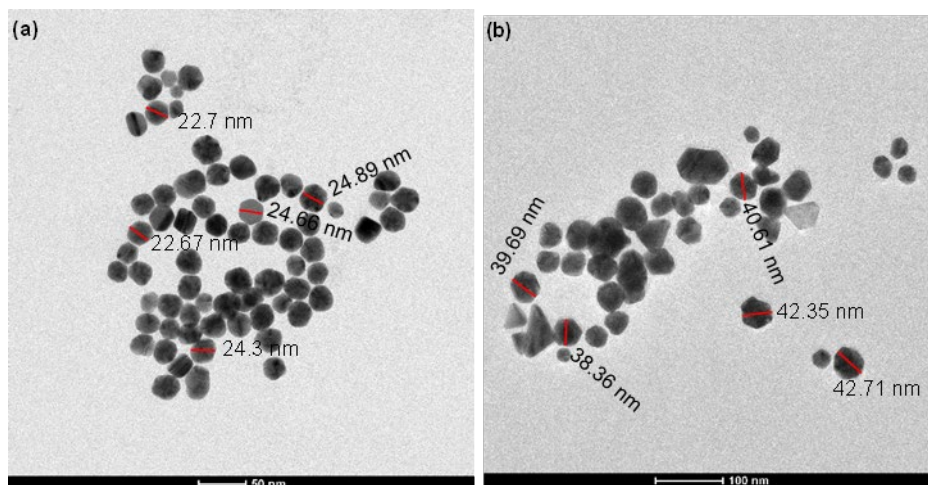


Fig 3. TEM images of (a) AuNPs α -CDs and (b) AuNPs β -CDs

metal ions. Several heavy metal ions such as Fe^{3+} , Mg^{2+} , Ni^{2+} , Cd^{2+} , Pb^{2+} , Cu^{2+} , Sn^{2+} , and Co^{2+} with a concentration of 10 ppm were added with AuNPs-CDs in a 1:1 ratio volume. The SPR of AuNPs α -CDs and AuNPs β -CDs before being added with metal ions are 524 nm. The only metal ions that changed the color and absorbance of AuNPs-CDs at 524 nm were Fe^{3+} [29-30]. The color of AuNPs α -CDs and AuNPs β -CDs were changed from bright pink to red and purple, respectively. The response time of color change by the addition of Fe^{3+} is about 2 s because there was a rapid color change when Fe^{3+} drops

into AuNPs (less than 1 min, rapid detection). Moreover, the change in color is visible to the naked eye (Fig. 4). On the other hand, the selectivity of AuNPs α -CDs and AuNPs β -CDs with the addition of several heavy metal ions. Some heavy metal ions did not change the absorbance of AuNPs α -CDs and AuNPs β -CDs at 524 nm. However, only Fe^{3+} increases the absorbance of the AuNPs α -CDs and AuNPs β -CDs at 524 nm from 0.18 to 0.37 and 0.23 to 0.39, respectively. This indicates that AuNPs α -CDs and AuNPs β -CDs are selective for detecting ion Fe^{3+} (Fig. 5).

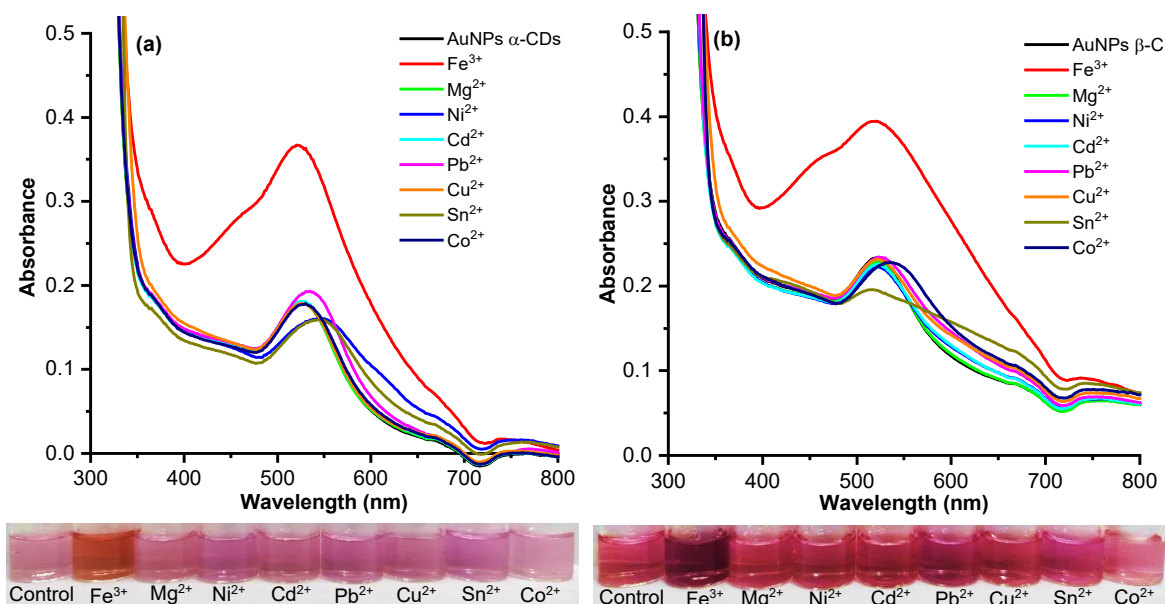


Fig 4. The UV-vis spectra of AuNPs using different stabilizer agents, (a) α -CDs and (b) β -CDs in the presence of various metal ions (10 ppm)

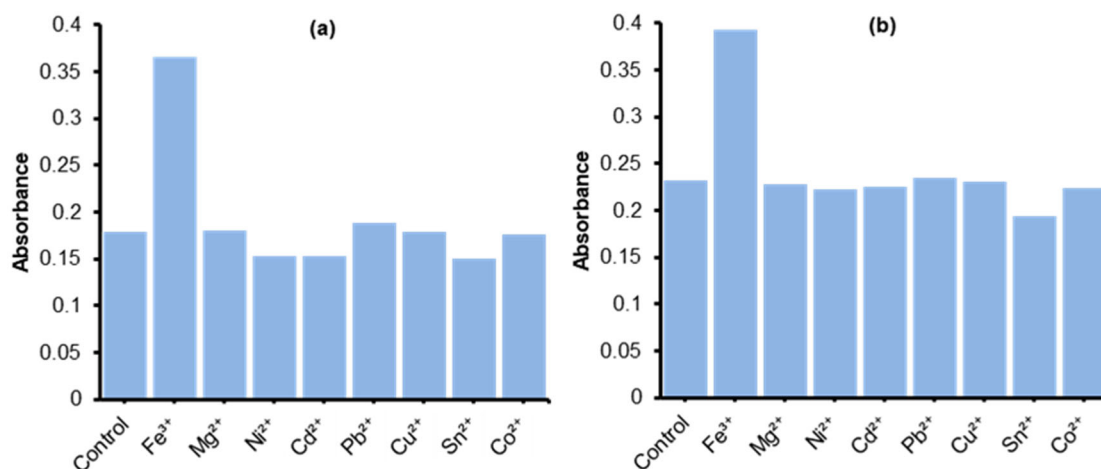


Fig 5. The selectivity of AuNPs in the presence of different stabilizers, (a) α -CDs and (b) β -CDs and metal ions concentration of 10 ppm from the absorbance data at 524 nm

Other Metal Ions Interference in the Reaction of AuNPs-CDs with Fe³⁺

The other metal ions were added, and their effects on the selectivity of AuNPs α -CDs or AuNPs β -CDs towards Fe³⁺ were investigated using a UV-vis spectrophotometer three times. It was shown that the absorbance of AuNPs α -CDs or AuNPs β -CDs with Fe³⁺ was not significantly affected by the addition of the other metal ions (Fig. 6). Thus, under the optimum conditions of Fe³⁺ sensing using AuNPs α -CDs or AuNPs β -CDs, the addition of other metal ions does not cause interference which proves good selectivity of AuNPs α -CDs or AuNPs β -CDs for colorimetric sensors of Fe³⁺.

Analytical Performance

The dynamic linear range of the calibration curve is one crucial factor to consider when assessing the effectiveness of AuNPs α -CDs and AuNPs β -CDs as colorimetric sensors of Fe³⁺. Changes in the absorbance (Δ Abs) of AuNPs α -CDs and AuNPs β -CDs at 524 nm towards the changes in Fe³⁺ concentration were monitored with UV-vis spectrometry. As the Fe³⁺ concentration increased, the color changed AuNPs α -CDs and AuNPs β -CDs to red and purple, respectively, and the absorbance at 524 nm increased. The Δ absorbance of AuNPs α -CDs and AuNPs β -CDs versus concentration of Fe³⁺ was plotted as a linear calibration

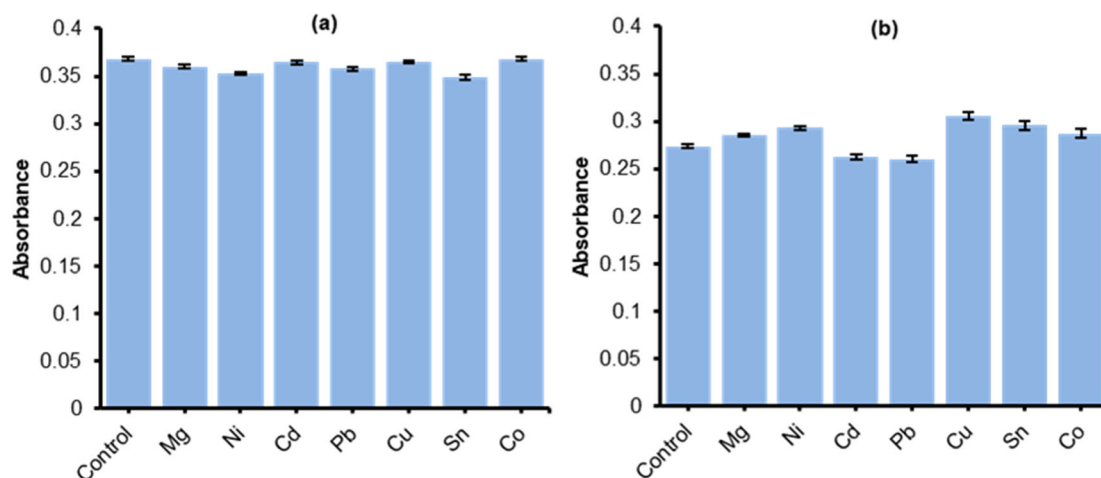


Fig 6. The interference of AuNPs in the presence of different stabilizers, (a) α -CDs and (b) β -CDs and metal ions concentration of 10 ppm from the absorbance data at 524 nm

plot in the range of 2–18 ppm. The rise in absorbance following the addition of Fe^{3+} is compared to the original absorbance before the addition of Fe^{3+} to determine Δ absorbance.

The calibration curve at 524 nm as a function of Fe^{3+} concentration is given in (Fig. 7). When the relationship between the absorbance of AuNPs and the concentration of Fe^{3+} is linear, this plot can be used to determine the level of Fe in the sample. The value of R^2 obtained was 0.996 for AuNPs α -CDs and 0.902 for AuNPs β -CDs with LoD 1.21 ppm, LoQ 4.02 ppm for AuNPs α -CDs and LoD 6.21 ppm, LoQ 20.72 ppm for AuNPs β -CDs, respectively. In the same concentration range, AuNPs α -CDs are more sensitive than AuNPs β -CDs evidenced by the LoD value of AuNPs α -CDs smaller than AuNPs β -CDs. Based on the same correlation coefficient (R^2) value obtained, it can be categorized into a good linear regression equation ($R^2 \geq 0.99$) for AuNPs α -CDs, so it is used for the detection of Fe^{3+} in tap water.

Table 1 shows the list time of analysis and the LoD for some colorimetric Fe^{3+} sensors developed based on SPR sensitivity as others [31-32]; it was more sensitive than other works [33-34]. The sensor developed here had the advantage of a short analysis time (less than 1 min). It proved that this research developed a Fe^{3+} colorimetric sensor that provided better sensitivity and rapid detection.

Precision and Recovery

The repeatability and reproducibility for colorimetric of AuNPs α -CDs and AuNPs β -CDs are given in Table 2. The repeatability of the sensor reflected the quality of sensor response and was investigated by measuring its absorbance at 524 nm in optimum conditions for 3.0 determination ($n = 3$) on the same day resulting in an acceptable relative standard deviation (RSD) lower than that determined by AOAC (7.3%) and Horwitz (11.3%) [35] confirms good repeatability. The

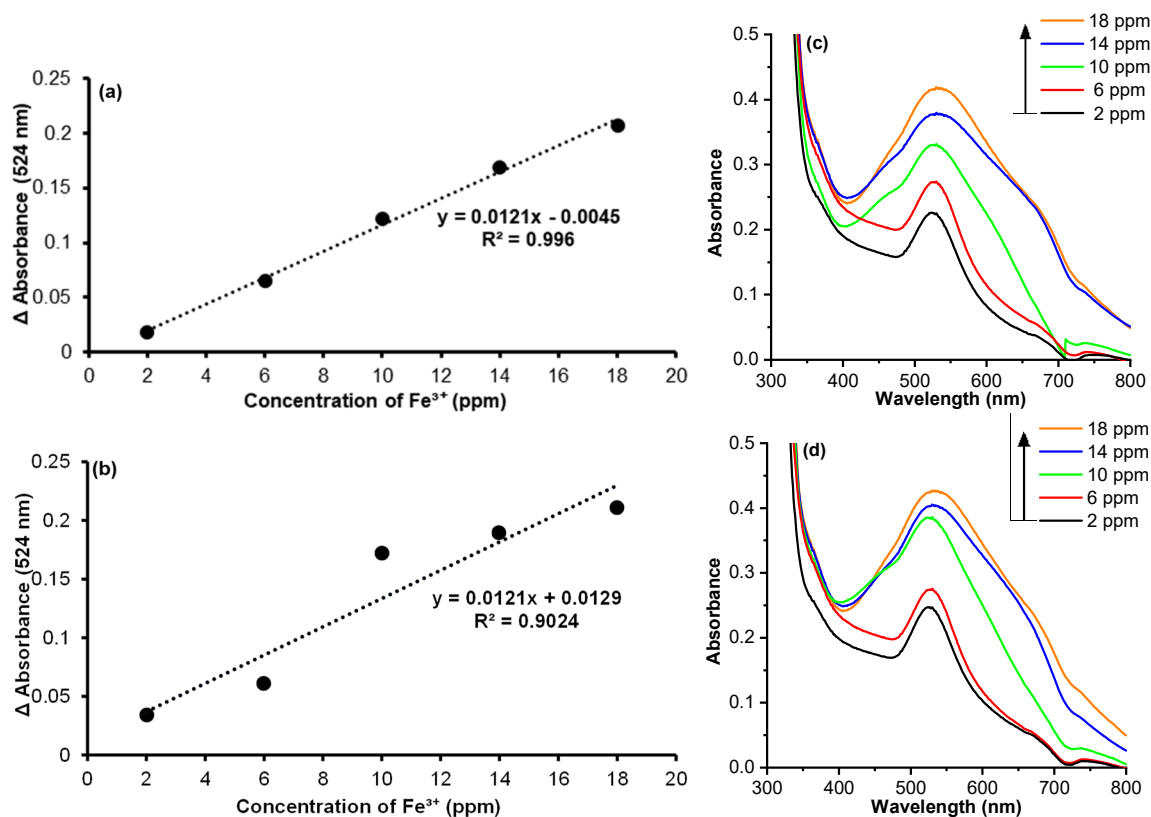


Fig 7. The linear relationship between the concentration of Fe^{3+} and Δ Absorbance of (a) AuNPs α -CDs and (b) AuNPs β -CDs at 524 nm. UV-vis Spectra of (c) AuNPs α -CDs and (d) AuNPs β -CDs with various concentrations of Fe^{3+} from 2 to 18 ppm

Table 1. Comparison of AuNPs α -CDs based UV-vis spectrometric method with the reported methods for detection of Fe^{3+}

Capping Reagents	Samples	Time of analysis	LoD	Ref.
pyrophosphate	Lake water samples	30 min	312 ng/mL	[31]
oxamic acid, <i>p</i> -aminobenzoic acid	Water, urine, and plasma samples	15 min	330 ng/mL	[32]
acidic thiourea mixture	-	15 min	50 ppm	[33]
ascorbic acid, some proteins and flavonoids from <i>Hibiscus cannabinus</i>	-	2 min	8.1 ppm	[34]
<i>o</i> -hydroxybenzoic acid and α - cyclodextrin	Tap water	< 1 min	1.2 ppm	This work

Table 2. Repeatability and reproducibility of (a) AuNPs α -CDs and (b) AuNPs β -CDs at 524 nm

(a)	Repeatability		Reproducibility	
	RSD (%)		RSD (%)	
Concentration Fe^{3+} (ppm)	AOAC	Horwitz	AOAC	Horwitz
2	0.02	1.80	6.63	1.80
6	0.32	1.53	4.30	1.53
10	0.18	1.41	1.29	1.41
14	0.45	1.34	2.40	1.34
18	0.06	1.29	3.32	1.29
(b)	Repeatability		Reproducibility	
	RSD (%)		RSD (%)	
Concentration Fe^{3+} (ppm)	AOAC	Horwitz	AOAC	Horwitz
2	0.03	1.80	4.12	1.80
6	0.10	1.53	4.15	1.53
10	0.06	1.41	0.86	1.41
14	0.02	1.34	1.46	1.34
18	0.05	1.29	0.93	1.29

reproducibility was examined at an absorbance of 524 nm in optimal conditions on different days so that the obtained RSD was lower than that determined by the AOAC (7.3%) and Horwitz (11.3%) [35] confirming good reproducibility.

AuNPs α -CDs are used in recovery because of their average size, shape uniformity, stability and sensitivity better than AuNPs β -CDs. Recovery tests with real samples were carried out using tap water taken at 3 different places in South Tangerang, Banten, Indonesia. Tap water samples were spiked with standard ion Fe^{3+} solutions (10 ppm) and then analyzed. The results summarized in (Table 3) demonstrated the recovery

range of 86.4 to 109.9% when compared with acceptable recovery percentages according to the concentration level of analyte in 10 ppm (80–110%) [35]. The results obtained are within that range so that the recovery results are acceptable and clearly confirm the applicability of the developed colorimetric sensor for the accurate determination of Fe^{3+} ions in tap water.

Reusability

The reusability of AuNPs α -CDs and β -CDs was carried out by adding EDTA which is commonly used as a binding agent or ligand for several metal ions or elements, especially Fe^{3+} . The use of EDTA is expected to bind Fe^{3+} ions so that AuNPs-CDs can be used again. In order to recover the initial absorbance from AuNPs α -CDs and β -CDs, the concentration EDTA for AuNPs α -CDs and β -CDs is 25 and 40 ppm, respectively. Further, the color change AuNPs α -CDs and AuNPs β -CDs after the addition of Fe^{3+} is red and purple, respectively.

Table 3. Recovery of AuNPs α -CDs for the analysis of Fe^{3+} in the samples

Samples	Spiked (ppm)	Detected by AAS (ppm)	Recovery (%)
Sample I	6.68	0.51	86.4
	8.05	0.51	92.4
Sample II	5.75	ND	97.8
	6.30	ND	93.7
Sample III	9.66	0.59	109.9
	10.52	0.59	105.1

ND: Not Detected is the content of Fe^{3+} is below the limit of detection (LoD) of AAS

The color change after the addition of EDTA in AuNPs α -CDs + Fe^{3+} and AuNPs β -CDs + Fe^{3+} was from red and purple to bright purple, respectively. The change in color and widening of the absorbance peaks indicate (Fig. 8) that the shape and size of the AuNPs α -CDs and β -CDs cannot return to their original shape and size. Thus, AuNPs α -CDs and β -CDs can be reused only twice (Fig. 9).

Application Test to Tap Water

The average size, shape uniformity, stability and sensitivity of AuNPs α -CDs are better than AuNPs β -CDs, so AuNPs α -CDs are chosen for application test to tap water. The analytical results of Fe^{3+} using the AuNPs α -CDs which were obtained by the proposed method, were not significantly different from those obtained by AAS, as shown in Table 4. That's because the correlations between the as-developed method and the AAS obtained t-test

values of 0.04; 0.52; and 0.04, respectively (the t-test value is 4.30 at a 95% confidence level); it is possible that the two methods did not reveal significantly different results. The outcomes of this application, therefore, demonstrated the applicability of the AuNPs α -CDs sensor method to the samples.

Characterization of AuNPs-CDs

TEM analysis

AuNPs α -CDs are used for test applications to tap water, so for characterization using TEM, only AuNPs

Table 4. Results of Fe^{3+} detection in samples of tap water

Samples	Developed method (ppm)	AAS (ppm)
Sample I	0.55	0.51
Sample II	0.52	ND
Sample III	0.55	0.59

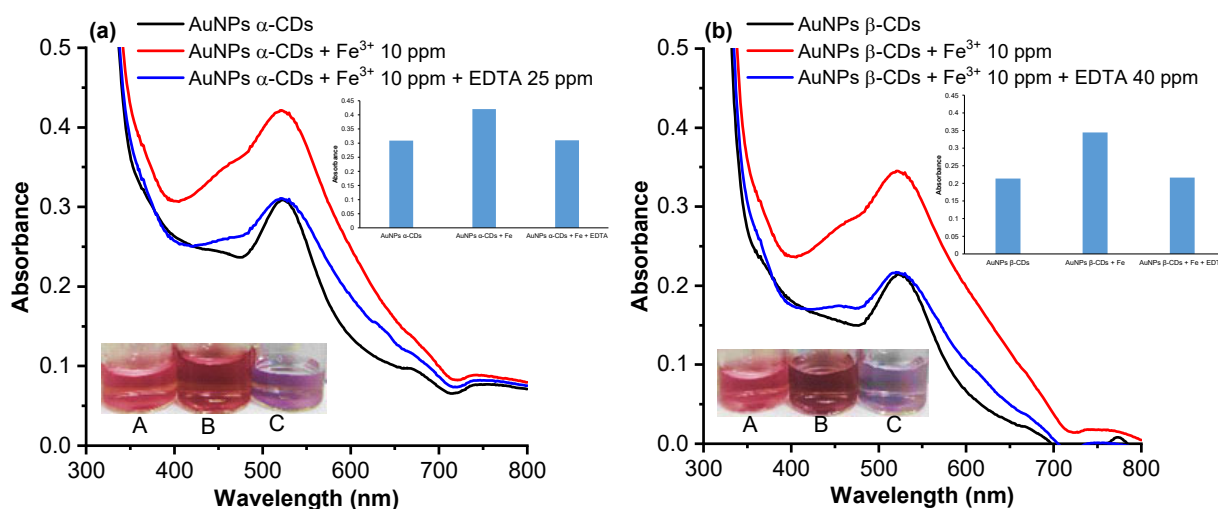


Fig 8. Reversibility of Fe^{3+} in the presence of various EDTA by using different stabilize agents, (a) α -CDs and (b) β -CDs. The color of AuNPs α -CDs and β -CDs (A) with change color after the addition of Fe^{3+} (B) and after the addition of EDTA (C). Bar diagram exhibiting magnitude of absorbance for reversibility as inset

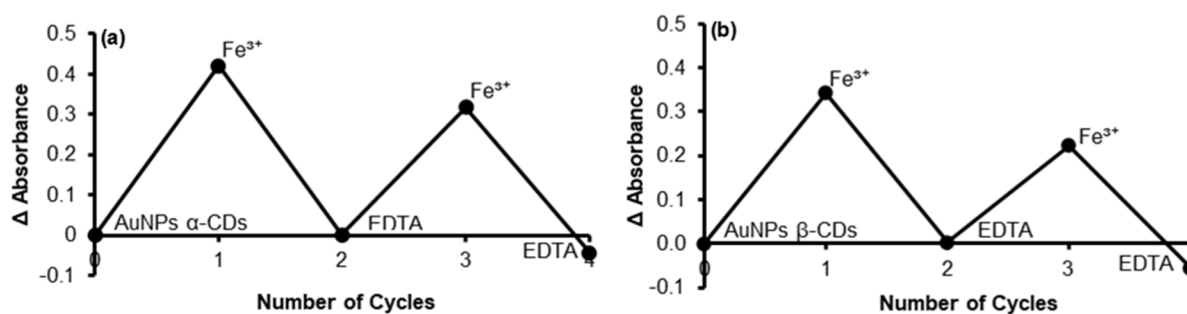


Fig 9. Reversible cycles of AuNPs α -CDs (a) and AuNPs β -CDs (b) addition with Fe^{3+} system with EDTA

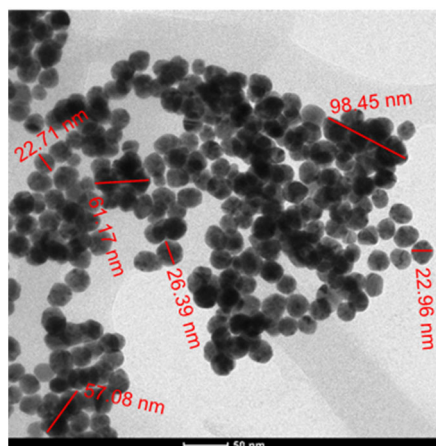


Fig 10. TEM images of the AuNPs α -CDs + Fe^{3+}

α -CDs + Fe^{3+} are used. The average results of nanoparticle size for AuNPs α -CDs + Fe^{3+} were 24.02 to 72.23 nm. The TEM images (Fig. 10) show that the presence of Fe^{3+} reduces the distance between the AuNPs α -CDs, but the AuNPs α -CDs retain their original shape, and aggregation occurs.

FTIR analysis

The IR spectra of AuNPs α -CDs and AuNPs α -CDs + Fe^{3+} (Fig. 11(a)) and AuNPs β -CDs and AuNPs β -CDs + Fe^{3+} (Fig. 11(b)) state an absorption peak which corresponded a C–H stretching + C–H (CH_2) stretching and C–H stretching at 2920 and 2860 cm^{-1} probably owned by cyclodextrin (α -CDs and β -CDs) [36]. Absorption peak which corresponded to a ketone C=O

stretching ortho for AuNPs α -CDs and AuNPs α -CDs + Fe^{3+} (Fig. 11(a)) at 1732 cm^{-1} , for AuNPs β -CDs at 1732 cm^{-1} and AuNPs β -CDs + Fe^{3+} at 1730 cm^{-1} , proved that *o*-HBA acts as a reducing agent and cyclodextrin acts as a stabilizer [37]. Stretching vibration of C=O carbonyl for AuNPs α -CDs and AuNPs β -CDs emerge at 1642 and 1643 cm^{-1} due to the presence of an electrostatic bond C=O with Au metal (Table 5). After the addition of Fe^{3+} (AuNPs α -CDs + Fe^{3+} and AuNPs β -CDs + Fe^{3+}), the wavenumber at the C=O stretching vibration carbonyl was shifted to 1647 and 1695 cm^{-1} . The shift of wavenumber was caused by the C=O carbonyl groups that were believed to bind with Fe^{3+} [37]. Other than that, O–H bending carbonyl and C=C stretching aromatic of AuNPs α -CDs and AuNPs β -CDs appeared at 1602 and 1452 cm^{-1} . After the addition of Fe^{3+} (AuNPs α -CDs + Fe^{3+}), the wavenumber at the O–H bending carbonyl and C=C stretching aromatic were shifted to 1608 and 1455 cm^{-1} , respectively. The shift of wavenumber was caused by the O–H bending carbonyl and C=C stretching aromatic to form bridges between AuNPs, causing a decrease in the distance among AuNPs α -CDs and AuNPs β -CDs. Therefore, the schematic between AuNPs α -CDs, AuNPs β -CDs, and Fe^{3+} based on FTIR results may be interpreted as shown in Scheme 1.

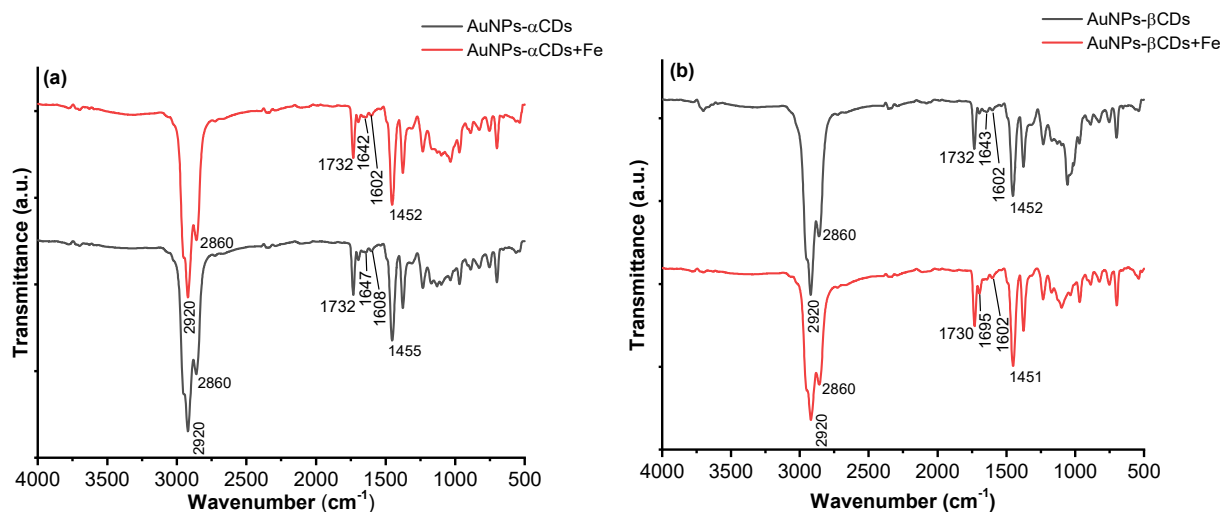
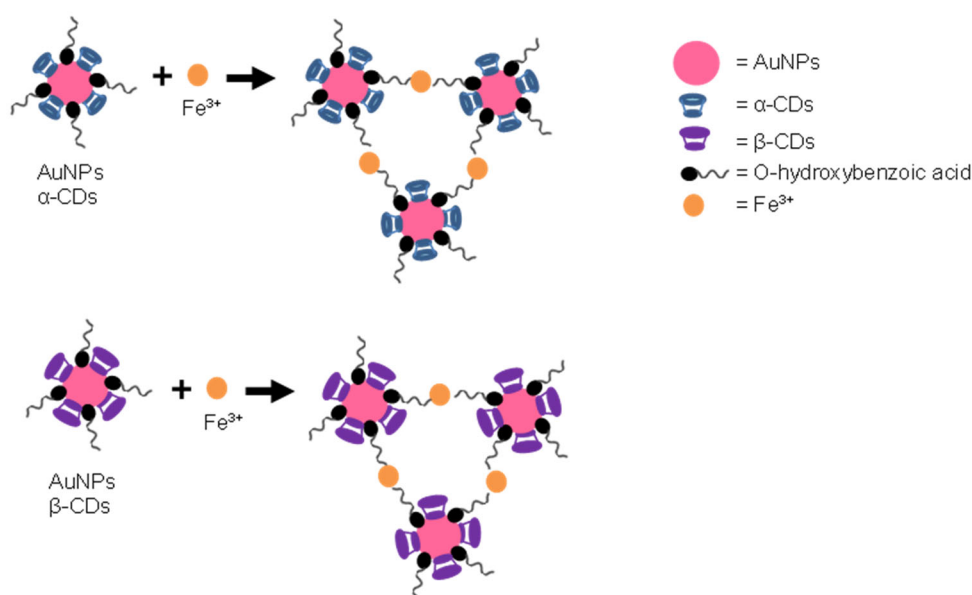


Fig 11. FTIR spectra of (a) AuNPs α -CDs and AuNPs α -CDs + Fe^{3+} and (b) AuNPs β -CDs and AuNPs β -CDs + Fe^{3+}

Table 5. Wavenumbers (cm^{-1}) of AuNPs CDs and AuNPs CDs- Fe^{3+} complexes

AuNPs α -CDs	AuNPs α -CDs + Fe^{3+}	AuNPs β -CDs	AuNPs β -CDs + Fe^{3+}	
2920	2920	2920	2920	C-H stretching + C-H (CH_2) stretching
2860	2860	2860	2860	C-H stretching
1732	1732	1732	1730	Ketone C=O stretching <i>ortho</i>
1642	1647	1643	1695	C=O stretching vibration carbonyl
1602	1608	1602	1602	O-H bending carbonyl
1452	1455	1452	1451	C=C stretching aromatic

**Scheme 1.** Scheme illustration of AuNPs AuNPs α -CDs and AuNPs β -CDs

CONCLUSION

This study's results indicated that AuNPs α -CDs were more stable than AuNPs β -CDs, with an absorbance drop of 17.76% at a 524 nm wavelength. With the average size of 23.34 nm, AuNPs α -CDs have a more consistent nanoparticle size and shape. The linear calibration curve at 524 nm's R^2 value of 0.996 with a LoD of 1.21 ppm and a LoQ of 4.02 ppm confirms the AuNPs α -CDs are more sensitive than AuNPs β -CDs. From this comparison, AuNPs α -CDs can be utilized to detect Fe^{3+} in tap water because it exhibits good precision, accuracy, and recovery.

ACKNOWLEDGMENTS

This research would like to acknowledge funding from the RIIM Gelombang 3 (2023) 12/II.7/HK/2023 and the facilities, scientific and technical supports from Advanced Characterization Laboratories Serpong, National

Research and Innovation Agency (BRIN) through *E-Layanan Sains, Badan Riset dan Inovasi Nasional*.

AUTHOR CONTRIBUTIONS

Adhi Maulana Yusuf: data curation, investigation, formal analysis, writing-original draft; Satrio Kuntolaksono: investigation, methodology, validation, supervision, and writing-review; Agustina Sus Andreani: conceptualization, formal analysis, funding acquisition, investigation, methodology, supervision, validation, writing-review & editing.

REFERENCES

- [1] Liang, W., Wang, G., Peng, C., Tan, J., Wan, J., Sun, P., Li, Q., Ji, X., Zhang, Q., Wu, Y., and Zhang, W., 2022, Recent advances of carbon-based nano zero valent iron for heavy metals remediation in soil and

- water: A critical review, *J. Hazard Mater.*, 426, 127993.
- [2] Amirjani, A., Kamani, P., Hosseini, H.R.M., and Sadrnezhaad, S.K., 2022, SPR-based assay kit for rapid determination of Pb^{2+} , *Anal. Chim. Acta*, 1220, 340030.
- [3] Li, H.Y., Zhao, S.N., Zang, S.Q., and Li, J., 2020, Functional metal-organic frameworks as effective sensors of gases and volatile compounds, *Chem. Soc. Rev.*, 49 (17), 6364–6401.
- [4] Zuo, Z., Song, X., Guo, D., Guo, Z., and Niu, Q., 2019, A dual responsive colorimetric/fluorescent turn-on sensor for highly selective, sensitive and fast detection of Fe^{3+} ions and its applications, *J. Photochem. Photobiol., A*, 382, 111876.
- [5] Tammina, S.K., Yang, D., Li, X., Koppala, S., and Yang, Y., 2019, High photoluminescent nitrogen and zinc doped carbon dots for sensing Fe^{3+} ions and temperature, *Spectrochim. Acta, Part A*, 222, 117141.
- [6] Amirjani, A., and Haghshenas, D.F., 2018, Ag nanostructures as the surface plasmon resonance (SPR)-based sensors: A mechanistic study with an emphasis on heavy metallic ions detection, *Sens. Actuators, B*, 273, 1768–1779.
- [7] Wu, Y., Pang, H., Liu, Y., Wang, X., Yu, S., Fu, D., Chen, J., and Wang, X., 2019, Environmental remediation of heavy metal ions by novel-nanomaterials: A review, *Environ. Pollut.*, 246, 608–620.
- [8] Liu, X., Li, N., Xu, M.M., Wang, J., Jiang, C., Song, G., and Wang, Y., 2018, Specific colorimetric detection of Fe^{3+} ions in aqueous solution by squaraine-based chemosensor, *RSC Adv.*, 8 (61), 34860–34866.
- [9] Wang, R., Jiao, L., Zhou, X., Guo, Z., Bian, H., and Dai, H., 2021, Highly fluorescent graphene quantum dots from biorefinery waste for tri-channel sensitive detection of Fe^{3+} ions, *J. Hazard. Mater.*, 412, 105962.
- [10] Xiong, X., Zhang, J., Wang, Z., Liu, C., Xiao, W., Han, J., and Shi, Q., 2020, Simultaneous multiplexed detection of protein and metal ions by a colorimetric microfluidic paper-based analytical device, *Biochip J.*, 14 (4), 429–437.
- [11] Soares, B.M., Santos, R.F., Bolzan, R.C., Muller, E.I., Primel, E.G., and Duarte, F.A., 2016, Simultaneous determination of iron and nickel in fluoropolymers by solid sampling high-resolution continuum source graphite furnace atomic absorption spectrometry, *Talanta*, 160, 454–460.
- [12] Lv, X., Man, H., Dong, L., Huang, J., and Wang, X., 2020, Preparation of highly crystalline nitrogen-doped carbon dots and their application in sequential fluorescent detection of Fe^{3+} and ascorbic acid, *Food Chem.*, 326, 126935.
- [13] Pang, L.Y., Wang, P., Gao, J.J., Wen, Y., and Liu, H., 2019, An active metal-organic anion framework with highly exposed SO_4^{2-} on {001} facets for the enhanced electrochemical detection of trace Fe^{3+} , *J. Electroanal. Chem.*, 836, 85–93.
- [14] Karami, C., Alizadeh, A., Taher, M.A., Hamidi, Z., and Bahrami, B., 2016, UV-visible spectroscopy detection of iron(III) ion on modified gold nanoparticles with a hydroxamic acid, *J. Appl. Spectrosc.*, 83 (4), 687–693.
- [15] Uzunoglu, D., Ergut, M., Kodaman, C.G., and Ozer, A., 2020, Biosynthesized silver nanoparticles for colorimetric detection of Fe^{3+} ions, *Arabian J. Sci. Eng.*, s13369-020-04760-8.
- [16] Chen, X., Zhao, Q., Zou, W., Qu, Q., and Wang, F., 2017, A colorimetric Fe^{3+} sensor based on an anionic poly(3,4-propylenedioxythiophene) derivative, *Sens. Actuators, B*, 244, 891–896.
- [17] Kumar, A., Zhang, X., and Liang, X.J., 2013, Gold nanoparticles: Emerging paradigm for targeted drug delivery system, *Biotechnol. Adv.*, 31 (5), 593–606.
- [18] Amirjani, A., and Fatmehsari, D.H., 2018, Colorimetric detection of ammonia using smartphones based on localized surface plasmon resonance of silver nanoparticles, *Talanta*, 176, 242–246.
- [19] Amirjani, A., Salehi, K., and Sadrnezhaad, S.K., 2022, Simple SPR-based colorimetric sensor to differentiate Mg^{2+} and Ca^{2+} in aqueous solutions, *Spectrochim. Acta, Part A*, 268, 120692.

- [20] Amirjani, A., Bagheri, M., Heydari, M., and Hesarak, S., 2016, Label-free surface plasmon resonance detection of hydrogen peroxide; A bio-inspired approach, *Sens. Actuators, B*, 227, 373–382.
- [21] Jansook, P., Ogawa, N., and Loftsson, T., 2018, Cyclodextrins: Structure, physicochemical properties and pharmaceutical applications, *Int. J. Pharm.*, 535 (1-2), 272–284.
- [22] Roy, N., Bomzan, P., and Nath Roy, M., 2020, Probing host-guest inclusion complexes of ambroxol hydrochloride with α - & β -cyclodextrins by physicochemical contrivance subsequently optimized by molecular modeling simulations, *Chem. Phys. Lett.*, 748, 137372.
- [23] Gopalan, P.R., 2010, Cyclodextrin-stabilized metal nanoparticles: Synthesis and characterization, *Int. J. Nanosci.*, 9 (5), 487–494.
- [24] Liu, Y., Male, K.B., Bouvrette, P., and Luong, J.H.T., 2003, Control of the size and distribution of gold nanoparticles by unmodified cyclodextrins, *Chem. Mater.*, 15 (22), 4172–4180.
- [25] Lakkakula, J.R., Divakaran, D., Thakur, M., Kumawat, M.K., and Srivastava, R., 2018, Cyclodextrin-stabilized gold nanoclusters for bioimaging and selective label-free intracellular sensing of Co^{2+} ions, *Sens. Actuators, B*, 262, 270–281.
- [26] Soomro, R.A., Nafady, A., Sirajuddin, S., Memon, N., Sherazi, T.H., and Kalwar, N.H., 2014, L-cysteine protected copper nanoparticles as colorimetric sensor for mercuric ions, *Talanta*, 130, 415–422.
- [27] Andreani, A.S., Kunarti, E.S., and Santosa, S.J., 2019, Synthesis of gold nanoparticles capped-benzoic acid derivative compounds (*o*-, *m*-, and *p*-hydroxybenzoic acid), *Indones. J. Chem.*, 19 (2), 376–385.
- [28] Ndikau, M., Noah, N.M., Andala, D.M., and Masika, E., 2017, Green synthesis and characterization of silver nanoparticles Using *Citrullus lanatus* fruit rind extract, *Int. J. Anal. Chem.*, 2017, 8108504.
- [29] Das, R., Sugimoto, H., Fujii, M., and Giri, P.K., 2020, Quantitative understanding of charge-transfer-mediated Fe^{3+} sensing and fast photoresponse by N-doped graphene quantum dots decorated on plasmonic Au nanoparticles, *ACS Appl. Mater. Interfaces*, 12 (4), 4755–4768.
- [30] Mohaghegh, N., Endo-Kimura, M., Wang, K., Wei, Z., Hassani Najafabadi, A., Zehtabi, F., Hosseinzadeh Kouchehbaghi, N., Sharma, S., Markowska-Szczupak, A., and Kowalska, E., 2023, Apatite-coated Ag/AgBr/ TiO_2 nanocomposites: Insights into the antimicrobial mechanism in the dark and under visible-light irradiation, *Appl. Surf. Sci.*, 617, 156574.
- [31] Wu, S.P., Chen, Y.P., and Sung, Y.M., 2011, Colorimetric detection of Fe^{3+} ions using pyrophosphate functionalized gold nanoparticles, *Analyst*, 136 (9), 1887–1891.
- [32] Buduru, P., and Reddy B.C., S.R., 2016, Oxamic acid and *p*-aminobenzoic acid functionalized gold nanoparticles as a probe for colorimetric detection of Fe^{3+} ion, *Sens. Actuators, B*, 237, 935–943.
- [33] Tripathy, S.K., Woo, J.Y., and Han, C.S., 2013, Colorimetric detection of Fe(III) ions using label-free gold nanoparticles and acidic thiourea mixture, *Sens. Actuators, B*, 181, 114–118.
- [34] Bindhu, M.R., and Umadevi, M., 2014, Green synthesized gold nanoparticles as a probe for the detection of Fe^{3+} ions in water, *J. Cluster Sci.*, 25 (4), 969–978.
- [35] González, A.G., Herrador, M.Á., and Asuero, A.G., 2010, Intra-laboratory assessment of method accuracy (trueness and precision) by using validation standards, *Talanta*, 82 (5), 1995–1998.
- [36] Hasanah, N., Manurung, R.V., Jenie, S.N.A., Indriyati, I., Prastya, M.E., and Andreani, A.S., 2023, The effect of size control of gold nanoparticles stabilized with α -cyclodextrin and β -cyclodextrin and their antibacterial activities, *Mater. Chem. Phys.*, 302, 127762.
- [37] Andreani, A.S., Kunarti, E.S., Hashimoto, T., Hayashita, T., and Santosa, S.J., 2021, Fast and selective colorimetric detection of Fe^{3+} based on gold nanoparticles capped with *ortho*-hydroxybenzoic acid, *J. Environ. Chem. Eng.*, 9 (5), 105962.